Journal of Physiology (2002), **543.3**, *pp.* 779–793
DOI: 10.1113/jphysiol.2002.024588

www.jphysiol.org

Journal of Physiology

A model of atropine-resistant theta oscillations in rat hippocampal area CA1

M. J. Gillies *, R. D. Traub ‡, F. E. N. LeBeau *, C. H. Davies †, T. Gloveli *, E. H. Buhl * and M. A. Whittington *

* *School of Biomedical Sciences, University of Leeds, Leeds LS2 9NQ, UK,* † *GlaxoSmithKline, Harlow, Essex, CM19 5AW, UK and* ‡ *Department of Physiology and Pharmacology, SUNY Health Science Center, Brooklyn, NY 11203, USA*

Theta frequency oscillations are a predominant feature of rhythmic activity in the hippocampus. We demonstrate that hippocampal area CA1 generates atropine-resistant theta population oscillations in response to metabotropic glutamate receptor activation under conditions of reduced AMPA receptor activation. This activity occurred in the absence of inputs from area CA3 and extra-ammonic areas. Field theta oscillations were co-expressed with pyramidal distal apical dendritic burst spiking and were temporally related to trains of IPSPs with slow kinetics. Pyramidal somatic responses showed theta oscillations consisted of compound inhibitory synaptic potentials with initial IPSPs with slow kinetics followed by trains of smaller, faster IPSPs. Pharmacological modulation of IPSPs altered the theta oscillation suggesting an inhibitory network origin. Somatic IPSPs, dendritic burst firing and stratum pyramidale interneuron activity were all temporally correlated with spiking in stratum oriens interneurons demonstrating intrinsic theta-frequency oscillations. Disruption of spiking in these interneurons was accompanied by a loss of both field theta and theta frequency IPSP trains. We suggest that population theta oscillations can be generated as a consequence of intrinsic theta frequency spiking activity in a subset of stratum oriens interneurons controlling electrogenesis in pyramidal cell apical dendrites.

(Resubmitted 20 May 2002; accepted after revision 2 July 2002; first published online 19 July 2002)
Corresponding author M. A. Whittington: School of Biomedical Sciences, The Worsley Building, University of Leeds, Leeds LS2 9NL, UK. Email: m.a.whittington@leeds.ac.uk

Field potential oscillations at theta frequencies (4–12 Hz) are readily observed in the hippocampal formation *in vivo* and have been implicated in various cognitive processes including processing of visuospatial information (O'Keefe & Nadel, 1978) and in models of memory formation and retrieval (Larson & Lynch, 1986; Buzsáki, 1989). Theta frequency oscillations are prominent in all areas of the hippocampal formation and, from lesion experiments, have been variously proposed to originate from reciprocal interactions between rhythmic inputs from the medial septum-diagonal band of Broca (MSDB), the entorhinal cortex and other subcortical structures (Petsche *et al.* 1962; Buzsáki *et al.* 1983; Vertes & Kocsis, 1997).

The majority of activity at theta frequencies observed in the hippocampal formation *in vivo* appears dependent on cholinergic activity and, more so, inputs from MSDB. However, recent findings concerning the MSDB have cast doubt on the notion that the MSDB alone has the capacity to impose a coherent theta frequency oscillation on the hippocampus (King *et al.* 1998). In addition data demonstrating the timing of hippocampal output activity with reference to excitatory and inhibitory inputs has revealed a complex relationship which is difficult to explain in terms of extrinsic control alone (see Buzsáki, 2002 for review).

In vitro models of theta frequency oscillations in hippocampal slices have demonstrated a number of situations in which the hippocampal formation alone may generate rhythmic activity within the theta range. Most of this work has used application of carbachol (with or without bicuculline) to generate theta-like discharges, particularly in area CA3, where they are attenuated by AMPA receptor blockers (MacVicar & Tse, 1989; Williams & Kauer, 1997). However, in this form of model, unlike *in vivo*, interneuron activity is not essential for rhythmogenesis (Traub *et al.* 1992). With inhibition intact, by far the most robust form of oscillation generated by carbachol in area CA3 is within the gamma band, with only weak activity at theta frequencies (Fisahn *et al.* 1998). *In vivo*, theta frequency oscillations are accompanied by a large amount of inhibitory interneuronal activity, with rhythmic trains of spikes from fast-spiking interneurons and suggested specific involvement of a number of interneuron subtypes in cornu ammonis oriens and lacunosum moleculare laminae and the dentate gyrus (Buzsáki, 2002).

Hippocampal interneurons are differentially sensitive to metabotropic glutamate receptor (mGluR)-dependent drive (e.g. van Hooft *et al.* 2000), and positive interactions between these receptors and the NMDA subtype of glutamate

receptor critical for theta genesis *in vivo* (Vanderwolf & Leung, 1983) have been reported (Awad *et al.* 2000). In addition co-activation of mGluRs and metabotropic cholinergic receptors has been reported to generate robust theta frequency oscillations in the hippocampus *in vitro* (Cobb *et al.* 2000). From this it was hypothesised that mGluR activation may also play a role in generating theta frequency oscillations in the hippocampus devoid of extrinsic, phasic inputs. We have previously shown that *transient* activation of metabotropic glutamate receptors in area CA1 of the hippocampus generates gamma frequency oscillations when AMPA receptor activation is blocked (Whittington *et al.* 1995). Here we demonstrate that *tonic* activation of metabotropic glutamate receptors also generates prominent, inhibition-based, theta frequency oscillations when AMPA receptor activation is attenuated or abolished.

METHODS

Male Wistar rats (~150 g) were fully anaesthetised with isoflurane prior to injection of ketamine (> 100 mg kg^{-1}) and xylazine (10 mg kg^{-1}), then cardioperfused with artificial cerebrospinal fluid (ACSF, containing (mM): NaCl, 126; KCl, 3; NaH_2PO_4, 1.25; $CaCl_2$, 2; $MgSO_4$, 2; $NaHCO_3$, 24; glucose, 10) in which NaCl had been replaced with an equiosmolar concentration of sucrose. All procedures were carried out in accordance with the UK Animals (Scientific Procedures) Act 1986. Transverse slices of mid hippocampus, 450 μm thick, were cut horizontally and maintained at the interface between oxygenated ACSF and humidified 95 % O_2–5 % CO_2 at 35 °C. CA1 minislices were obtained by dissecting transverse slices between CA3 and CA1 subfields.

Extracellular recordings were made via Neurolog amplifiers (Digitimer, UK) using glass microelectrodes containing ACSF (resistance < 3 MΩ). Potentials were band pass filtered on-line (0.1 Hz–2 kHz). Intracellular recordings were made via Axoclamp amplifiers (Axon Instruments, Inc., Union City, CA, USA) using glass microelectrodes containing either potassium methylsulfate or potassium acetate (resistance 60–100 MΩ). Stratum oriens interneurons demonstrated diverse electrophysiological characteristics. The data presented are from a subset of oriens interneurons which showed brief action potentials, large, compound afterhyperpolarisations (AHPs) and intrinsic theta frequency membrane potential oscillations in the absence of drug application ($n = 11$). Stratum pyramidale interneurons were more homogeneous in their electrophysiological properties and demonstrated brief spikes, large, brief AHPs and fast firing rates on depolarising current injection with little accommodation ($n = 3$). Apical pyramidal neuronal dendrites were impaled > 200 μm from stratum pyramidale and were identified by their low amplitude action potentials, small AHPs and burst generation on injection of depolarising current ($n = 7$). In addition pyramidal cells were also recorded at the level of the soma ($n = 25$). All drugs were bath applied at known concentrations: DHPG ((*S*)-3,5-dihydroxyphenylglycine), 20–200 μM; NBQX (2,3-dioxo-6-nitro-1,2,3,4-tetrahydrobenzo[f]quinoxaline-7-sulfonamide), 20 μM; carbachol, 20 μM; AP5 (D-(−)-2-amino-5-phosphonopentanoic acid), 50 μM; atropine, 10 μM; bicuculline, 30 μM; CGP55845 ((2*S*)-3-[[(1*S*)-1-(3,4-dichlorophenyl)ethyl]amino-2-hydroxypropyl](phenylmethyl) phosphinic acid), 1 μM; diazepam, 1–10 μM; and thiopental, 50 μM. Drugs were obtained from Tocris (Bristol, UK) or Sigma (Poole, UK).

Peak frequency of recorded activity was determined off-line from digitised data (digitisation frequency 10 kHz) from power spectra of 60 s epochs of recorded activity. Patterns of spike timing were illustrated by superimposition of concurrently recorded stratum pyramidale field potential and intracellular electrode signal. Average spike timing profiles were quantified by combining cross correlograms of 3 s epochs of data from concurrently recorded stratum pyramidale field potentials and intracellular signals. Correlation values were calculated by measuring the *y*-axis distance between the first negative and first positive peaks to the right of the central peak of the correlograms. IPSP rise times were measured using Minianalysis (Synaptosoft Inc.). More than 600 IPSPs were measured from each slice used in the analysis. Decay time measurements could only be estimated owing to the compound nature of the inhibitory events.

RESULTS

AMPA receptor blockade transforms gamma into theta frequency oscillation

Gamma frequency oscillations were generated in area CA1 of rat hippocampal slices by bath application of DHPG (20–200 μM). Stratum pyramidale field recordings showed a peak in power spectra of 37 ± 9 μV^2 Hz^{-1} at a mean frequency of 37 ± 2 Hz ($n = 29$). In each case the resulting gamma oscillations were modulated at theta frequencies either weakly or not at all (Fig. 1*A*). However, bath application of NBQX (20 μM) abolished field power in the gamma band ($P < 0.001$, $n = 29$) and increased dramatically the power in the upper theta band (6–12 Hz). Peak power increased from 22 ± 7 μV^2 Hz^{-1} to 115 ± 43 μV^2 Hz^{-1} at a mean peak frequency of 6.7 ± 0.3 Hz ($n = 29$). Autocorrelations demonstrated clear rhythmicity at theta frequencies (Fig. 1*A*). Laminar profiles ($n = 4$) revealed a clear phase reversal between distal stratum radiatum/lacunosum moleculare and other laminae (Fig. 1*B*). Similar AMPA receptor blockade-dependent expression of field theta oscillations in area CA1 were seen with bath application of carbachol (20–40 μM) and NBQX or kainate (1.0–1.5 μM) and the specific AMPA receptor blocker SYM2206 (10 μM) (data not shown). Activity in the theta band was also apparent in CA1 mini-slices where CA3 and hilar inputs were surgically removed (data not shown). Mean peak power in the theta band was not significantly different in CA1-only slices compared with intact hippocampal slices ($P = 0.19$, $n = 6$).

The AMPA blockade-dependent expression of theta frequency field oscillations in area CA1 was in stark contrast to the pattern of rhythmogenesis in area CA3 (Fig. 1*C*). Theta frequency oscillations were more prominent in area CA3 compared with CA1 in the absence of AMPA receptor blockade, but were attenuated concurrently with gamma oscillations on bath application of NBQX as shown previously (MacVicar & Tse, 1989). In the presence of DHPG alone peak power within the theta band in area

CA3 was 115 ± 30 μV^2 Hz^{-1} at a mean frequency of 7.5 ± 0.3 Hz ($n = 4$). On addition of NBQX this fell to 9.2 ± 0.8 μV^2 Hz^{-1} ($P < 0.05$).

mGluR-induced theta frequency oscillations are atropine resistant and involve inhibition

The field theta frequency oscillations generated by DHPG in the absence of AMPA receptor-mediated fast excitation were resistant to the muscarinic acetylcholine receptor antagonist atropine (10 μM). Mean peak amplitude was 41 ± 12 μV^2 Hz^{-1} at a mean frequency of 7.3 ± 0.5 Hz ($n = 7$) in controls and 45 ± 11 μV^2 Hz^{-1} ($n = 7$, $P > 0.05$) in the presence of atropine (Fig. 2*Ab*). This was in contrast to theta-band oscillations generated in area CA1 with carbachol, in the presence of NBQX, which were significantly reduced in the presence of atropine (control peak power 96 ± 41 μV^2 Hz^{-1}, with atropine 19 ± 11 μV^2 Hz^{-1} ($n = 5$, $P < 0.05$, Fig. 2*Ab*). Cholinergically and glutamatergically generated theta frequency oscillations were differentially modified by bath application of the NMDA receptor antagonist AP5 (50 μM). mGluR driven oscillations were almost abolished with AP5 (peak theta power with DHPG was 45 ± 9 μV^2 Hz^{-1}, with DHPG + AP5 14 ± 2 μV^2 Hz^{-1} ($n = 5$, $P < 0.05$). Muscarinic AchR-driven oscillations were also significantly reduced (carbachol 76 ± 42 μV^2 Hz^{-1} and carbachol + AP5 40 ± 19 μV^2 Hz^{-1} ($n = 5$, $P < 0.05$, Fig. 2*Aa*). However, theta oscillations remaining in the presence of carbachol and AP5 showed a significantly lower peak frequency (control, 8.5 ± 0.4 Hz; with AP5, 4.8 ± 0.2 Hz ($P < 0.05$).

Atropine-resistant field theta oscillations were modified by some $GABA_A$ receptor modulators, but not by the $GABA_B$ receptor antagonist CGP55845 (1 μM). In control conditions theta power was 45 ± 10 μV^2 Hz^{-1}, in the presence of CGP55845 this value was 37 ± 6 μV^2 Hz^{-1} ($n = 8$, $P > 0.05$). Bicuculline almost abolished power at theta frequencies ($P < 0.05$, $n = 6$, Fig. 2*Ba*), whereas diazepam (1 μM, $n = 6$) significantly reduced peak frequency ($P < 0.05$) without affecting peak amplitude ($P > 0.05$; Fig. 2*Bb*). Thiopental (50 μM) had no significant effect on peak frequency or amplitude of oscillation ($P > 0.05$, $n = 6$).

IPSPs are compartmentally distributed

The above data on the effects of drugs acting on the $GABA_A$ receptor suggested an essential role of $GABA_A$ receptor-mediated synaptic inhibition in rhythmogenesis at theta frequencies. This was investigated further using somatic intracellular recordings from CA1 pyramidal neurons (Fig. 3). During gamma oscillations pyramidal cell somatic membrane potentials fluctuate at gamma frequencies owing to a barrage of fast $GABA_A$ receptor-mediated IPSPs. These IPSPs were fairly homogeneous both in amplitude and rise time, with a tight distribution of estimated rise times around 2.2 ms (Fig. 3*C*). After complete blockade of AMPA receptor-mediated fast excitation smaller trains of often compound IPSPs with similar rise times were still

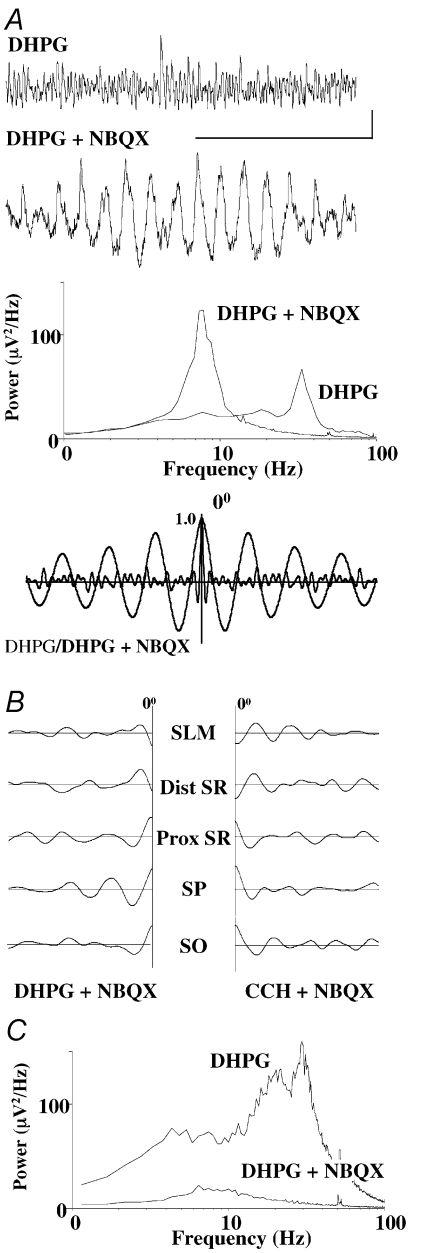

Figure 1. Reduction in AMPA receptor-mediated drive exposes theta field oscillations driven by metabotropic receptors

A, DHPG, 20–200 μM, generates gamma oscillations in area CA1. Blockade of AMPA receptors with 20 μM NBQX transforms the field gamma oscillation into a field theta oscillation. Example traces show field potentials from CA1 stratum pyramidale. Scale bars: 1 s, 50 μV. Power spectra (60 s epochs) show large increase in power within the theta band. Autocorrelations show frequency differences in the field oscillation before and after NBQX administration. *B*, laminar profile of theta field potentials reveals a sharp phase reversal in distal stratum radiatum. Data shown are cross correlations (−0.5 to 0.5 s) using two electrodes: a reference electrode in stratum pyramidale and a roving electrode positioned as indicated. *C*, DHPG, 20–100 μM, generates gamma/theta oscillations in area CA3. Power spectra (60 s epochs, $n = 5$) show power in both gamma and theta bands. Bath application of NBQX 20 μM leaves only a small peak at theta frequencies in contrast to the effects in area CA1.

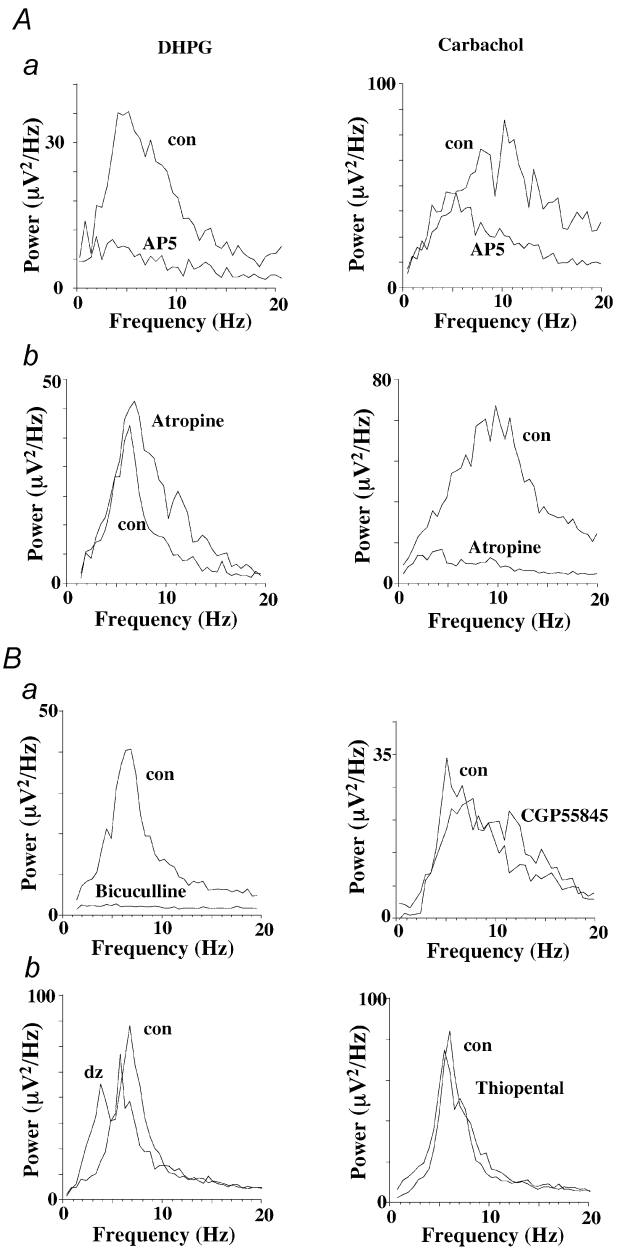

Figure 2. Pharmacology of theta field oscillations generated by DHPG and carbachol, in the presence of NBQX

A, both mGluR and mAchR mediated theta oscillations are attenuated by NMDA receptor blockade. *Aa*, mean power spectra ($n = 5$) for theta oscillations generated by DHPG or carbachol. Bath application of 50 μM D-AP5 almost abolished power in the theta band for mGluR-mediated oscillations and significantly reduced theta power during mAchR-mediated oscillation (see text). *Ab*, mean power spectra ($n = 5$) showing slight enhancement of theta activity generated by mGluR activation in the presence of atropine (10 μM) and abolition of theta activity generated by mAchR activation. *B*, effects of GABA receptor modulators on mGluR-mediated theta oscillations. *Ba*, blockade of $GABA_A$ receptors with bicuculline (30 μM) abolishes theta activity ($n = 6$) whereas blockade of $GABA_B$ receptors with CGP55845 (1 μM, $n = 4$) had no effect. *Bb*, diazepam (1 μM) reduced the mean peak frequency of the oscillation and enhanced power in the lower theta range ($n = 7$) whereas thiopental had no significant effect ($n = 6$).

seen at gamma frequencies but an additional class of IPSP was also seen with rise times longer than those seen during a pure gamma oscillation (Fig. 3*C*). Rise times for IPSPs during gamma oscillations were 2.2 ± 0.6 ms. The distribution of rise times during field theta-band oscillations was bimodal with the values for the slower, larger IPSPs having a mean of 6.5 ± 1.7 ms ($P < 0.05$, $n = 6$ cells from six slices recorded at −30 mV). Estimated decay times of these slower IPSPS were also longer than those seen during gamma oscillations. IPSP decays during field gamma oscillations were 15.2 ± 3.1 ms, whereas the estimated decay time constants for the slower IPSPs visible during field theta oscillations were 27 ± 6 ms. These slower IPSPs occurred at theta frequencies and were strongly correlated with concurrent field recordings (Fig. 3*A*). Mean phase lead between peak IPSP and stratum pyramidale field potential peak was 12 ± 5 ms.

The range of rise times seen was broad and the slow kinetics suggested a possible dendritic origin. Distal apical dendritic recordings (> 200 μm from stratum pyramidale) revealed the presence of these slower IPSPs during theta oscillations *and* during field gamma oscillations when dendrites were artificially depolarised to −30 mV (Figs 3*B* and 6*B*).

Theta frequency oscillations in stratum oriens interneurons are associated with inhibition and hyperpolarisation-activated current (I_h)

At least two subtypes of inhibitory interneuron within area CA1 (oriens lacunosum-moleculare and lacunosum moleculare interneurons) are capable of generating intrinsic theta frequency firing patterns with projections to mid- and distal-pyramidal cell apical dendrites (Chapman & Lacaille, 1999; Maccaferri *et al.* 2000). Given the pharmacological profile of the field theta oscillation (see below) we examined the role of stratum oriens interneurons demonstrating intrinsic theta frequency oscillatory activity in the population theta-band activity observed. Cells were impaled in the outer one-third of stratum oriens close to the alveus. Fast spiking cells with no intrinsic membrane theta oscillation impaled in this region ($n = 3$) were rejected from the study. The remaining 11 theta-generating interneurons had a membrane potential and input resistance during field theta oscillations of −59 ± 5 mV and 40 ± 5 MΩ, respectively.

Spiking was seen spontaneously but sporadically in each of the above interneurons at resting membrane potential. In each case injection of depolarising current (+0.05 to +0.15 nA) induced tonic firing at theta frequencies (Fig. 4*A*). Bath application of 50 μM DHPG (or DHPG and 20 μM NBQX) tonically depolarised these interneurons to an average resting potential of −53 ± 3 mV and induced a robust firing pattern at theta frequencies (Fig. 4*B*). Spike triggered averaging showed a theta frequency pattern of

Journal of Physiology

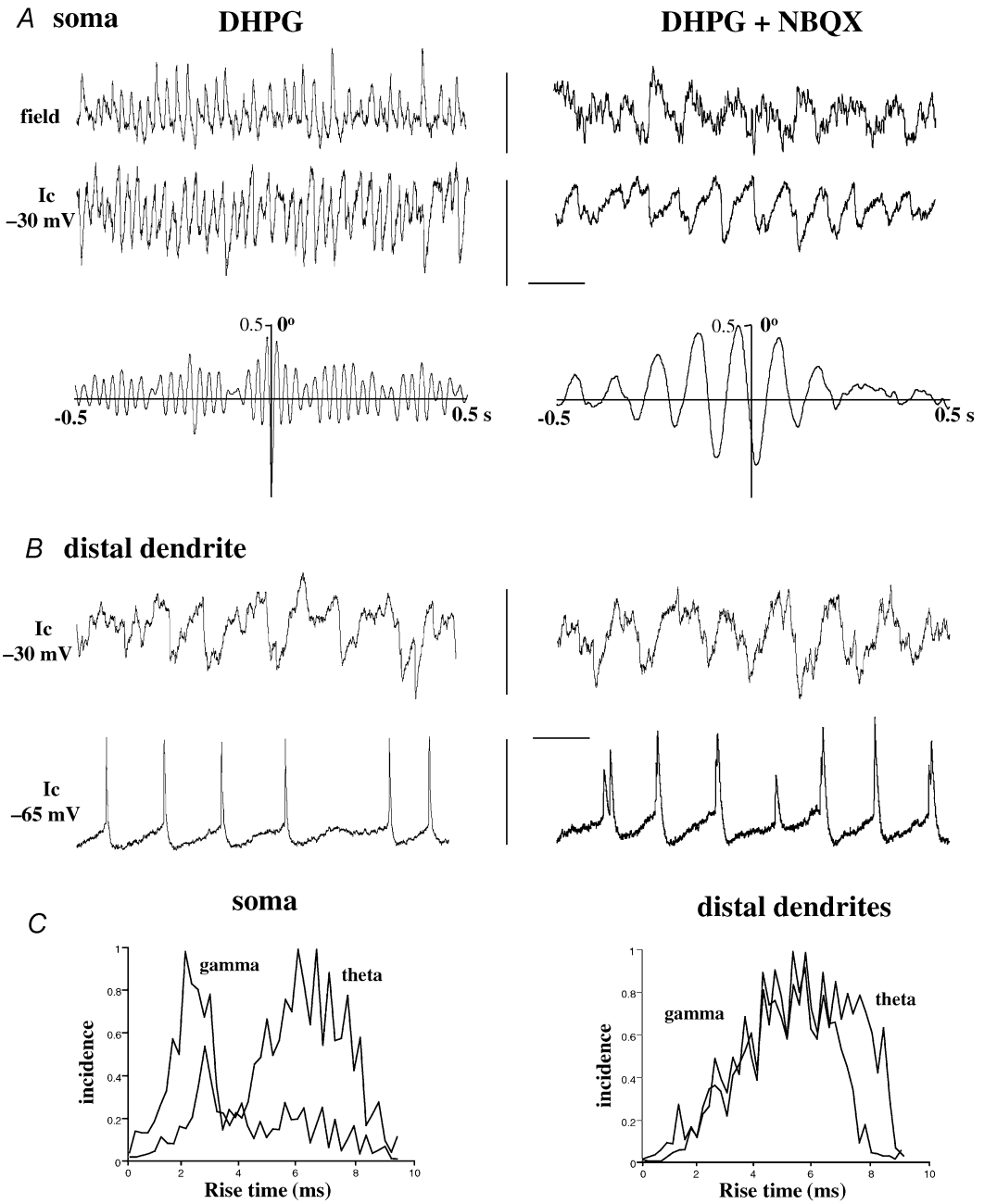

Figure 3. Pyramidal cell distal apical dendrites are active at theta frequencies during field gamma and field theta oscillations

A, concurrent CA1 stratum pyramidale field and somatic intracellular recordings of gamma and theta oscillations induced by DHPG and DHPG + NBQX, respectively. Gamma oscillations are expressed as a rhythmic train of IPSPs with fast kinetics (frequency 35–60 Hz). IPSP trains are negatively correlated with the local field potential and show no phase lag/lead (lower traces). Theta oscillations are also expressed as rhythmic trains of IPSPs with slower kinetics (see Fig. 4, frequency 4–11 Hz). IPSP trains at theta frequency are negatively correlated with the local field potential with a phase lag of 4–6 ms. Scale bars: 100 μV (field), 5 mV (Ic), 100 ms. *B*, distal apical dendritic recordings (> 250 μm from stratum pyramidale) during field/somatic gamma oscillations demonstrate rhythmic IPSPs at theta frequencies (3–10 Hz) at −30 mV. At more negative membrane potentials theta oscillations are observed as trains of small amplitude (6 ± 3 mV) broad spikes. During field/somatic theta oscillations distal dendrites also show trains of IPSPs at theta frequencies and complex fast spike events at theta frequencies at more hyperpolarised membrane potentials. Scale bars: 5 mV (−30 mV), 10 mV (−65 mV), 100 ms. *C*, histograms of distribution of IPSP rise times observed in somatic and distal apical dendritic compartments during gamma or theta field oscillations. Data shown as mean distributions for > 600 individual IPSPs per recording (n > 4 in each condition).

action potential generation and power spectra (60 s epochs) revealed a strong output at theta frequencies. Hyperpolarisation of recorded interneurons by injection of −0.1 to −0.2 nA current produced a transient hyperpolarisation and cessation of spiking. However, this hyperpolarisation decayed in the continued presence of negative current injection (τ = 1.5 ± 0.3 s and theta frequency spiking was restored after 3–5 s (Fig. 4*Ba*). This suggested the possibility that tonic firing was maintained, at least in part, by a hyperpolarising activated current. Bath application of the I_h blocker ZD7288 (10 μM) produced a small (2–3 mV) hyperpolarisation of interneurons and abolished all spontaneous spiking (Fig. 4*C*). Injection of depolarising current in the presence of ZD7288 restored spiking in these cells but rhythmicity was absent.

During field gamma oscillations, induced by DHPG, these interneurons received IPSPs at gamma frequency (Fig. 5*A*). Cross correlations showed that IPSP trains appeared approximately in antiphase to the local field gamma oscillation at the level of stratum pyramidale. In the absence of current injection, in the presence of DHPG alone, these oriens interneurons were tonically active but fired only at theta frequencies despite the inhibitory gamma-frequency input (Fig. 5*B*). During field theta oscillations interneurons continued to fire action potentials at theta frequencies but in a more temporally precise manner (autocorrelations, Fig. 5*B*). IPSP trains in these interneurons during field theta-band activity were tightly temporally correlated with the local field potential as seen for pyramidal IPSPs (mean phase lead for IPSP peak

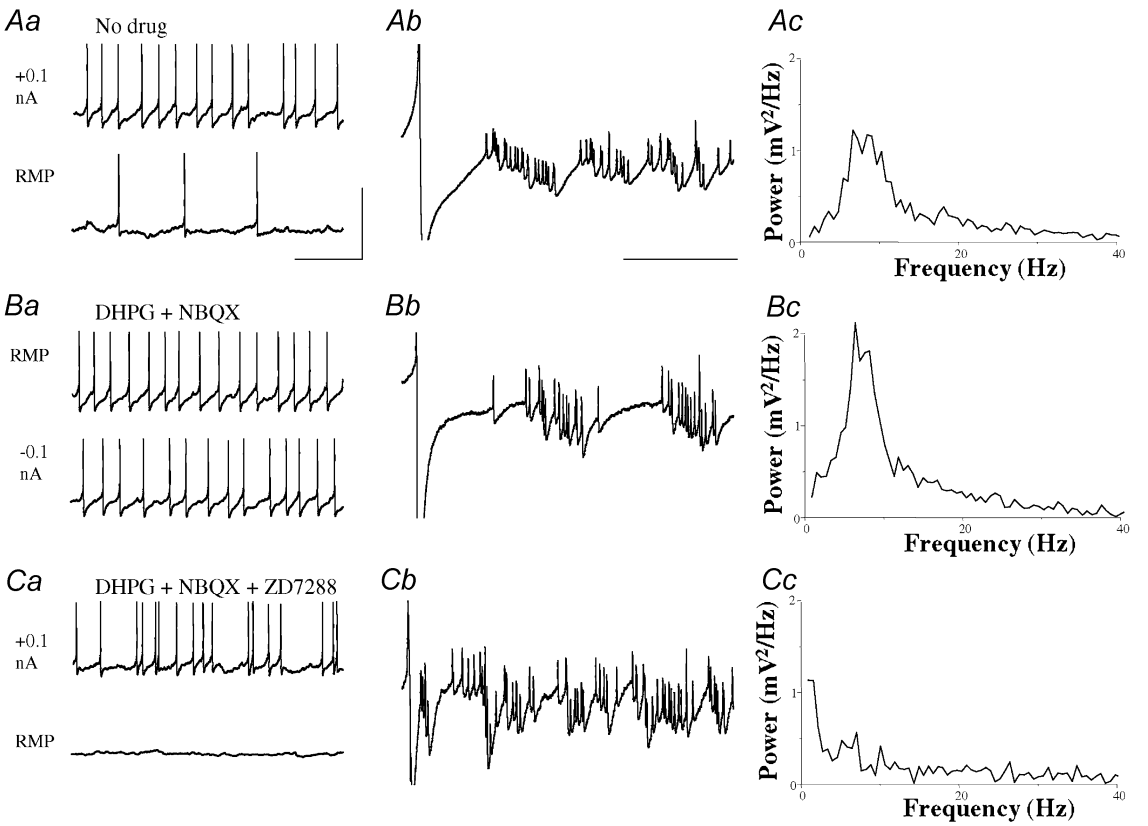

Figure 4. Stratum oriens interneurons generate theta frequency spiking

Aa, spiking in oriens interneurons in the absence of drug. Example traces show data from one oriens interneuron at resting membrane potential (RMP = −59 mV) and during +0.1 nA current injection. Scale bars: 50 mV, 0.5 s. *Ab*, spike triggered averages of 20 consecutive periods during injection of +0.1 nA current. Scale bar: 100 ms. *Ac*, power spectrum of 60 epoch of data from a cell during depolarising current injection as in *Aa* and *Ab*. *Ba*, spiking in oriens interneurons in the presence of DHPG, 50 μM and NBQX, 20 μM. Example traces show data from one oriens interneuron at resting membrane potential (RMP = −54 mV) and during −0.1 nA hyperpolarising current injection following recovery of spiking (see results). Scale bars: 50 mV, 0.5 s. *Bb*, spike triggered averages of 20 consecutive periods during RMP. Scale bar: 100 ms. *Bc*, power spectrum of 60 epoch of data from a cell during depolarising current injection as in *Ba* and *Bb*. *Ca*, spiking in oriens interneurons is disrupted by ZD7288, 10 μM. Example traces show data from one oriens interneuron at resting membrane potential (RMP = −56 mV) and during +0.1 nA current injection. Scale bars: 50 mV, 0.5 s. *Cb*, spike triggered averages of 20 consecutive periods during injection of +0.1 nA current. Scale bar: 100 ms. *Cc*, power spectrum of 60 epoch of data from a cell during depolarising current injection as in *Ca* and *Cb*.

Journal of Physiology

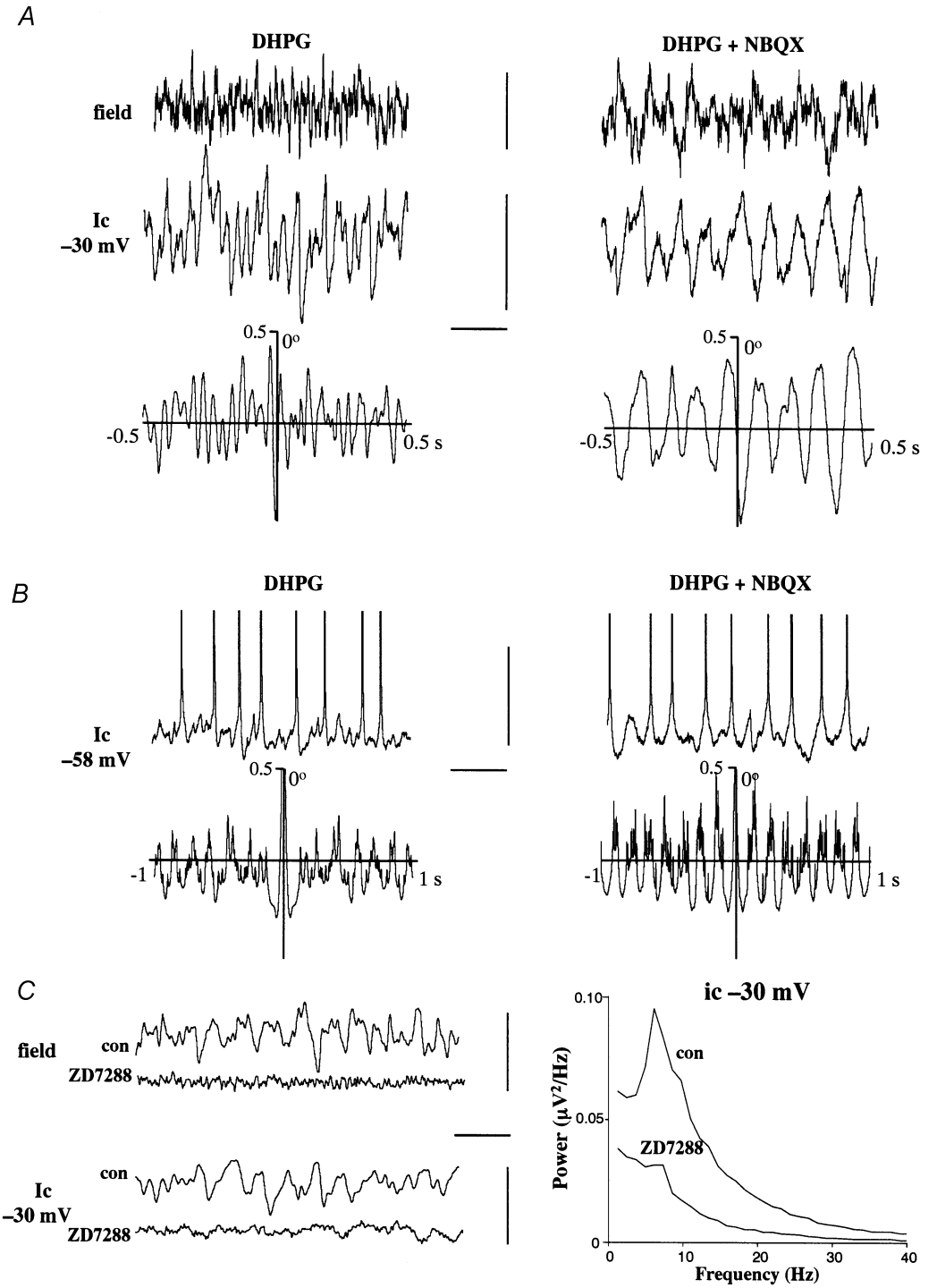

Figure 5. Theta activity in stratum oriens interneurons

A, concurrent stratum pyramidale field potential and intracellular interneuron recordings during gamma oscillation (DHPG) and theta oscillations (DHPG + NBQX). Intracellular recordings taken from artificially depolarised neurons at −30 V. Scale bars: 0.1 mV (field), 5 mV (I_c −30 mV), 200 ms. Below are cross correlograms showing phase relationship between interneuron IPSPs and field theta oscillations. *B,* spiking in interneurons during gamma (DHPG) and theta (DHPG + NBQX) oscillations at resting membrane potential. Note spiking occurs at theta frequencies in both cases, spikes truncated for clarity. However, autocorrelograms reveal more rhythmic theta spiking during field theta than during field gamma oscillations. Scale bars: 10 mV, 200 ms. *C,* 10 μM ZD7288 blocks both field theta oscillations and trains of slow IPSPs onto interneurons recorded at −30 mV membrane potential. Power spectra from pooled data from five slices (five interneurons) demonstrate almost complete abolition of theta frequency IPSPs. Scale bars: 100 μV (field), 10 mV (I_c −30 mV), 200 ms.

Journal of Physiology

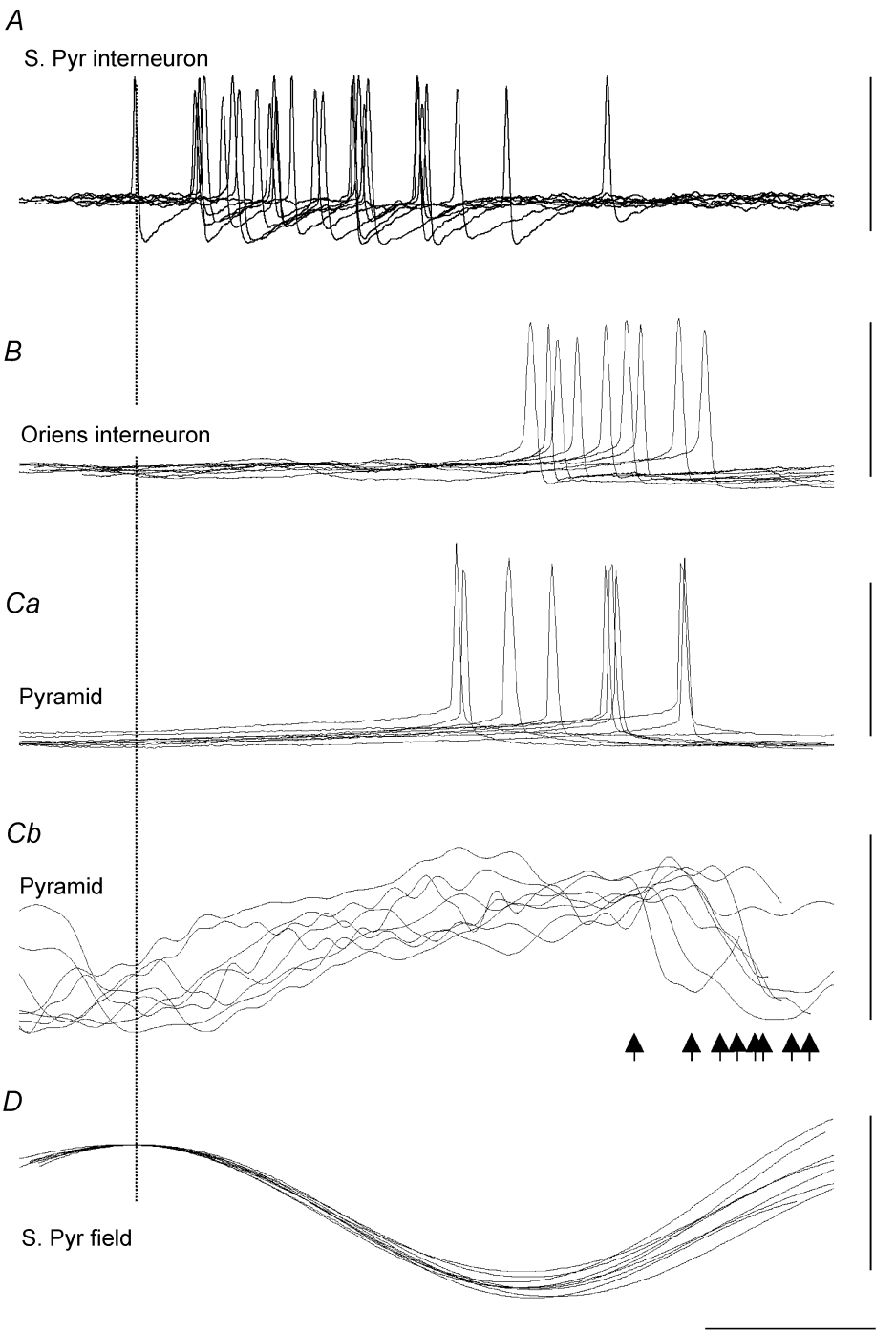

Figure 6. Compound somatic IPSPs temporally correlate with both stratum oriens and stratum pyramidale interneuron spiking

Overlaid traces from nine consecutive theta periods aligned with the peak upward deflection in concurrently recorded stratum pyramidale field potentials. *A,* stratum radiatum, fast spiking, interneurons generated bursts of action potentials during the descending phase of the field theta oscillation. *B,* stratum oriens theta interneurons generated single action potentials on the initial rising phase of the field theta oscillation. *Ca*, pyramidal cell soma (injected with 0.2 nA depolarising current) generated single action potentials within a period towards the end of action potential generation in stratum pyramidale interneurons and the beginning of action potential generation in oriens theta interneurons. *Cb*, subthreshold membrane potential oscillations in pyramidal cell soma in the absence of current injection reveal compound IPSPs phase locked to the concurrently recorded field (*D*). The initial peaks of the IPSPs are marked with arrows and occurred just before, or during, peak upward deflection in the field recording (see also Fig. 3*A* right panel cross correlation). Scale bars: 20 ms, 60 mV (*A*, *B*, *Ca*), 2 mV (*Cb*), 0.4 mV (*D*).

compared to peak upward deflection in the stratum pyramidale field was 11 ± 4 ms (n = 5, Fig. 5*A*, cf. phase relationship for IPSPs in pyramidal cells in Fig. 3*A*). They consisted of compound inhibitory events with individual components having estimated kinetics similar to those seen in pyramidal neuronal apical dendrites (data not shown).

Disruption of the hyperpolarisation-activated current I_h has been shown to disrupt spike generation in the 'O-LM' subclass of oriens interneuron, but not in LM-interneuron theta generators (Maccaferri & McBain, 1996; Chapman & Lacaille, 1999). In addition to testing the role of I_h in the theta-generating oriens interneurons (above), we also examined the effects on field theta oscillations. Bath application of ZD7288 (10 μM) had no significant effect on field gamma oscillations (n = 5, data not shown) but abolished the theta frequency pattern of pyramidal IPSPs, and abolished the field theta oscillation itself (Fig. 5*C*). These data suggested that intrinsic theta frequency spiking properties of these interneurons were critical to the generation of CA1 population theta oscillations.

Action potential timing during theta frequency oscillations

We examined the firing relationships of pyramidal neurons and stratum pyramidale interneurons relative to the activity in oriens theta generating interneurons described above during field theta frequency activity. Intracellular recordings from stratum pyramidale interneurons, pyramidal cells and oriens interneurons were temporally aligned to the concurrently recorded stratum pyramidale field potential (band pass filtered at 0.1–15 Hz, Fig. 5). Trains of action potentials in stratum pyramidale interneurons at a

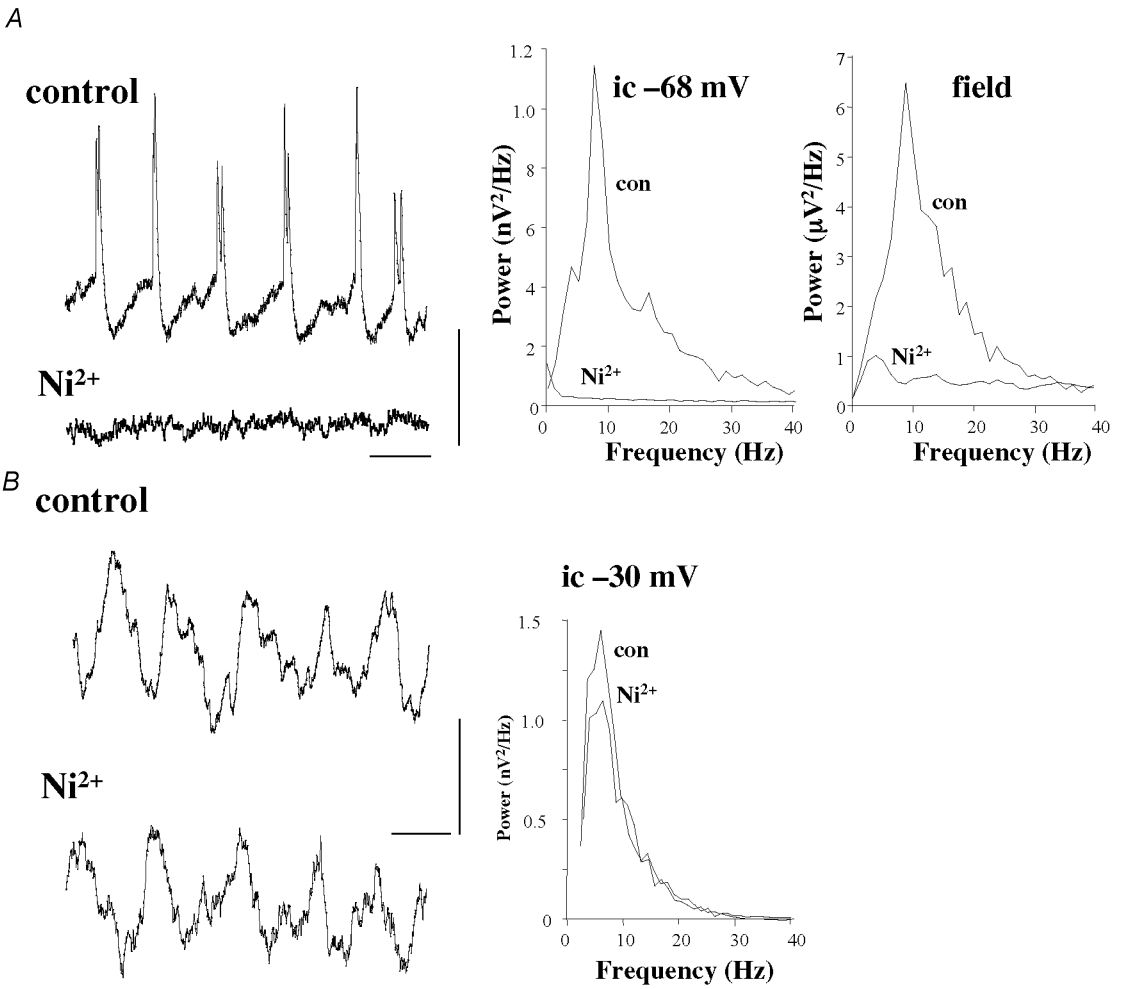

Figure 7. Expression of field theta oscillations generated by DHPG and NBQX is dependent on dendritic electrogenesis

A, nickel ions (0.1 mM) block both distal dendritic spike generation and the field theta oscillation. Example traces show a train of spikes at theta frequency recorded at a membrane potential of −68 mV before and after bath application of 0.1 mM Ni^{2+}. Power spectra show abolition of field theta power and theta activity in distal dendrites. Scale bars: 5 mV, 100 ms. *B*, depolarisation of distal dendrites reveals trains of slow IPSPs at theta frequency. Blockade of field theta and dendritic electrogenesis with Ni^{2+} failed to alter theta-frequency IPSP activity. Scale bars: 5 mV, 100 ms.

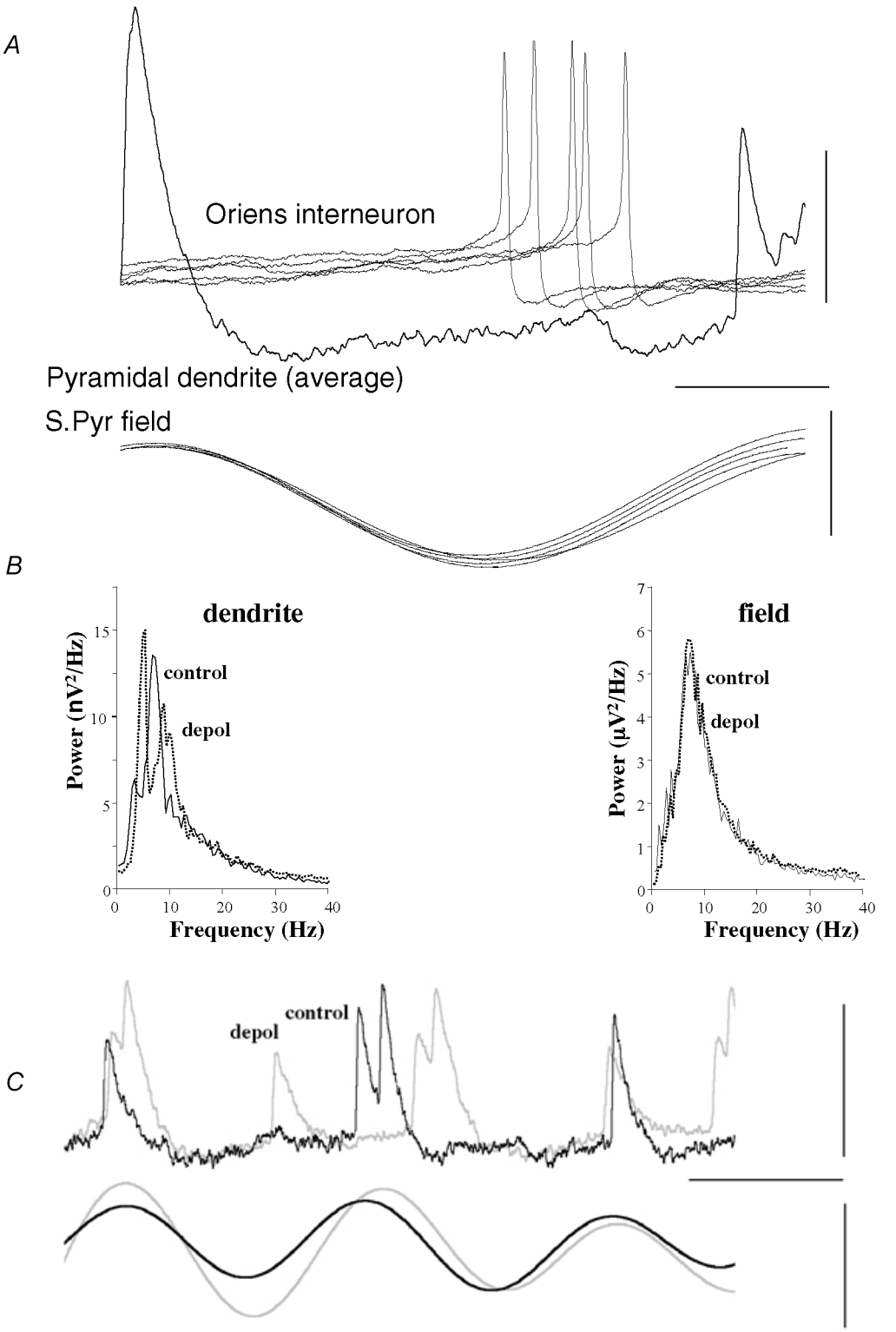

Figure 8. Timing of dendritic bursts is controlled by IPSPs

A, dendritic spike-triggered average of five periods of a theta oscillation recorded in a pyramidal apical dendrite with concurrent stratum pyramidale field recording (band pass 0.1–15 Hz). Traces are aligned to the peak upward deflection of the field to demonstrate correlation between dendritic burst firing and somatic field positivity. Note AHP prolonged by IPSPs peaking 62–71 ms after the onset of the previous burst (see also Fig. 7*A*). Five consecutive periods of oriens interneuron activity are also superimposed (and aligned to the concurrently recorded field potential) to illustrate the relationship between the IPSP timing and interneuron output. Scale bars: 20 ms, 5 mV (dendrite), 30 mV (oriens interneuron), 0.3 mV (field). *B*, depolarising current injection (0.1–0.3 nA) into dendrites disrupted dendritic burst timing in a manner

frequencies of 45–80 Hz were seen on the descending phase of the field theta oscillation (Fig. 6*A*. $n = 3$). The number of spikes per theta period ranged from zero to five with at least one spike generated per 0.92 periods of field theta frequency activity. Cessation of stratum pyramidale interneuron firing corresponded temporally with the generation of a single spike in stratum oriens theta interneurons (Fig. 6*B*). Cross correlation of stratum oriens theta cell firing and field theta oscillation at the level of stratum pyramidale demonstrated a mean phase lead of oriens cell spiking of 24 ± 9 ms ($n = 5$) compared with field peak. Pyramidal cell somatic firing was seen in only 1/25 cells recorded but could be elicited with injection of tonic depolarising current (0.1–0.2 nA). In these conditions pyramidal cells fired one spike per field theta period during the trough of the field oscillation, i.e. towards the end of the train of str. pyramidale interneuron spikes and approximately concurrent with the firing of a spike in str. oriens theta cells (Fig. 6*Ca*). Analysis of the subthreshold membrane potential oscillations at the level of the pyramidal neuronal soma revealed compound IPSPs with initial peak negativity seen on the upward phase of the field oscillation approximately 10 ms after oriens theta cell action potential generation. The tail of these IPSPs appear prolonged by smaller IPSPs during the period when str. pyramidale interneurons generated trains of action potentials (see Fig. 9, Discussion).

Field theta frequency oscillations are expressed through dendritic electrogenesis

The above sequence of spikes and IPSPs demonstrated that pyramidal neuronal somatic membrane potential changes were strongly correlated with the field theta oscillation but with a fixed phase angle compared to peak str. pyramidale field potential. Stratum pyramidale interneurons fired action potentials with a broad range of phase leads cf. the stratum pyramidale field. Stratum oriens interneurons fired single action potentials with a phase lead of *ca* 25 ms and the large, slow IPSPs seen in oriens interneurons and pyramidal cells were seen to peak 10–15 ms before the peak of the stratum pyramidale field. These observations suggested that the pattern of membrane potential changes in pyramidal neurons and interneurons could not be directly responsible for the observed field potential picked up by the extracellular recording electrode. However, abolition of rhythmic outputs from oriens interneurons was shown to abolish the field theta band oscillations.

We next investigated how this apparent discrepancy between the timing of interneuron outputs and field theta oscillations could occur. The answer appeared to involve pyramidal dendritic electrogenesis: During both field gamma and theta oscillations dendrites at membrane potentials between −70 and −60 mV generated small amplitude spikes at theta frequencies. The spikes seen during theta frequency oscillations were modified from those seen during gamma oscillations and often consisted of single or double spikes of a longer duration (Fig. 7*A*, cf. Fig. 3*B*). During theta oscillations these dendritic spikes were strongly correlated with the local field oscillation. Cross correlations showed a mean phase difference of +3 ± 7 ms ($n = 5$) when comparing peak dendritic positivity with the peak of the stratum pyramidale field oscillation (data not shown), i.e. because of the phase reversal of the field theta oscillation along the apical dendritic axis (Fig. 1*B*) dendritic spikes corresponded temporally to the troughs in distal stratum radiatum field theta frequency oscillations.

If these dendritic spikes were responsible for the expression of the field theta frequency oscillation then their blockade should abolish the field oscillation while leaving the pattern of intracellularly recorded theta frequency IPSPs intact. Nickel ions have been shown to selectively abolish dendritic calcium spikes of similar spatial origin, kinetics and voltage-dependence to those seen here (Isomura *et al.* 2002). These authors also demonstrated that nickel did not affect somatic bursting, nor did it effect synaptic transmission significantly. Bath application of Ni^{2+} (0.1 mM) completely abolished these spikes during theta activity (Fig. 7*A*). Ablation of dendritic spiking was accompanied by an almost complete abolition of power in the theta frequency range in field recordings ($P < 0.05$, $n = 5$). However, abolition of dendritic spiking and the field theta oscillation did not affect the trains of slow IPSPs recorded in pyramidal cell dendrites. Depolarisation of dendrites to −30 mV revealed a persistence of inhibitory synaptic input at theta frequencies (Fig. 7*B*) suggesting that, although expression of field theta oscillations was dependent on pyramidal dendritic electrogenesis, the pattern of inhibitory input to pyramidal cells at theta frequencies was not.

Dendritic periodicity involves both AHPs and IPSPs

The above observations indicated that nickel-sensitive dendritic spiking showed the correct spatiotemporal characteristics to be considered a candidate for the origin

consistent with breakdown of IPSP-mediated AHP prolongation. Mean power spectra show data ($n = 5$) from experiments with depolarisation (depol.) and without (control). Note split peak in spectra from depolarised dendrites. Mean field spectra (right panel) from stratum pyramidale potentials recorded concurrently with dendrites showed no change in field theta power on depolarisation of a single pyramidal apical dendrite. *C*, example traces illustrate the effect of depolarisation on dendritic burst firing. Depolarising current injection induced burst firing on the tail of the previous burst AHP before IPSP onset. The resulting dual periodicity corresponded with the two peaks in the power spectra. Scale bars: 60 ms, 10 mV (dendrite, upper traces), 0.4 mV (field, lower traces).

of the field theta oscillation. However, this still left a discrepancy between the timing of interneuron outputs at theta frequency and the timing of dendritic spikes/population theta band activity. In this model it seemed unlikely that local theta synchrony and periodicity was controlled by the kinetics of network IPSPs (unlike gamma oscillations (Whittington *et al.* 1995)). The slowest kinetics seen were for IPSPs that appeared to originate from oriens interneurons (20–30 ms), and these interneurons fired action potentials approximately 25 ms before the peak of the stratum pyramidale field and the dendritic spikes. However, analysis of subthreshold dendritic membrane potential changes between spikes revealed a biphasic hyperpolarising wave (Fig. 8*A*, cf. also Fig. 7*A*). This suggested that factors other than the dendritic IPSP played a role in the timing of dendritic spikes.

We hypothesised that the slow dendritic IPSPs were acting to prolong the intrinsic afterhyperpolarisation (AHP) following a dendritic burst. Thus dendritic spikes were generated not on the slow rebound of the previous spikes AHP, but on the more rapid rebound from the IPSP. If this was the case then depolarisation of the recorded dendrite by injection of current should allow the dendrite to reach threshold for spike generation earlier in the AHP–IPSP sequence. If this depolarisation were sufficient to initiate a dendritic spike before IPSP invasion then this should shift the pattern of generation of dendritic spikes away from control by the IPSP and towards control by the AHP. Evidence for this was seen when comparing mean power spectra ($n = 5$) of concurrently recorded stratum pyramidale field theta oscillations and the accompanying dendritic spiking (Fig. 8). With non-depolarised dendrites spiking occurred after a small IPSP which occurred in time with the oriens interneuron output (Fig. 8*A*). In this mode dendritic spiking occurred temporally coordinated with, and at the same frequency as, the field oscillation (Fig. 8*B* and *C*). However, when the recorded dendrites were depolarised (+0.1 to +0.2 nA) the spectrum peak was split with bimodal peaks occurring at slower and faster frequencies when compared to the concurrent field (Fig. 8*B*). Analysis of dendritic recordings showed that depolarisation resulted in two periodicities for spike generation, one corresponding to decay from the spike AHP and one corresponding to decay from the AHP and the theta frequency IPSP (Fig. 8*C*). Thus dendritic spiking is temporally coordinated by the network IPSP input, with spiking occurring on the rebound from dendritic IPSPs apparently generated by oriens interneurons. These observations also indicate that the degree of dendritic depolarisation in individual pyramidal cells controlled the periodicity of the dendritic spiking with reference to the local population theta frequency oscillation.

DISCUSSION

These data demonstrate that metabotropic glutamate receptor activation in area CA1 of the hippocampal slice preparation generates a field oscillation with a frequency in the high-theta band (6–10 Hz). This frequency range corresponded to that observed in the awake rat, but not that seen for atropine-sensitive theta (2–5 Hz; Buzsáki, 2002). The pharmacology of this field oscillation revealed a rhythm which was independent of muscarinic cholinergic receptor drive, strongly dependent on NMDA receptor and $GABA_A$ receptor activity and expressed as a field potential oscillation by pyramidal cell dendritic electrogenesis.

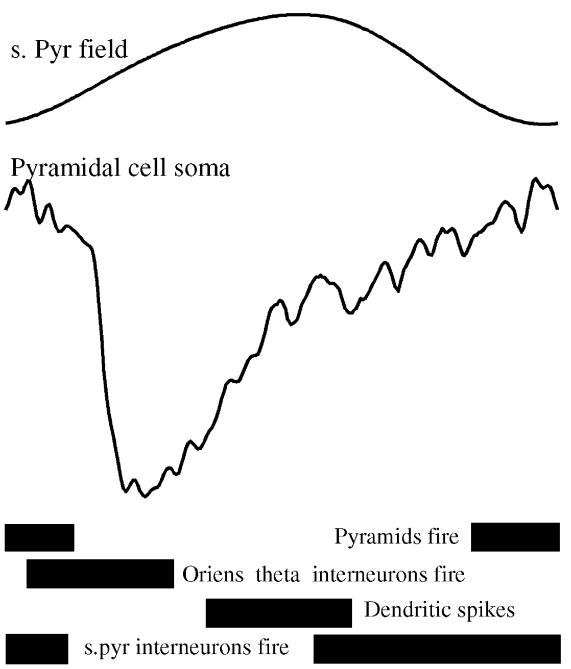

Figure 9. Relationship between pyramidal cell somatic compound IPSP and neuronal electrogenesis

Schematic representation of the procession of action potential generation in pyramidal cell soma, stratum pyramidale and stratum oriens 'theta' interneurons, and burst firing in apical dendrites. The figure shows a single period of theta oscillation with concurrently recorded stratum pyramidale field potential (band pass filtered 0.1–15 Hz) and pyramidal somatic membrane potential change. The compound IPSP consists of an initial, large, IPSP temporally correlated with the period of oriens 'theta' interneuron firing. This is then interrupted by a small depolarising hump temporally correlated to dendritic electrogenesis and is terminated by a train of small, faster IPSPs temporally correlated with action potential generation in stratum pyramidale interneurons. Spontaneous pyramidal somatic action potential generation rarely occurred but injection of depolarising current generated action potentials at the peak of the membrane potential positivity (i.e. towards the end of the train of small IPSPs) corresponding to the peak downward deflection in the stratum pyramidale field potential.

The key mechanism of generation of theta frequency population activity in this model appeared to involve intrinsic theta frequency membrane potential oscillations in a subset of stratum oriens interneurons. Blockade of I_h has been shown to disrupt their intrinsic pattern of action potential generation in some oriens interneurons (Maccafferi & McBain, 1996) and markedly disrupts theta frequency IPSP trains both in these interneurons and in pyramidal cells in the present model. During blockade of AMPA receptor-mediated fast excitatory synaptic transmission, coherent action potential generation in these interneurons at theta frequency appeared to provide temporal organisation to the rhythmic electrogenic activity of stratum pyramidale apical dendrites. However, this was demonstrated not to be a reciprocal arrangement as blockage of this dendritic electrogenesis with nickel ions preserved the pattern of dendritic IPSP invasion at theta frequencies.

The blockade of AMPA receptors was a critical requirement of the experimental conditions needed to see this population theta activity. This situation was clearly different to previous models of theta oscillation *in vitro* where CA3 was the target region (MacVicar & Tse, 1989; Cobb *et al.*1995; Williams & Kauer, 1997), and limits the model as a useful *in vitro* tool with which to study signal processing in area CA1 during theta rhythms. However, theta oscillations were observed intracellularly in the dendritic compartment even during field gamma oscillations (with AMPA receptor-mediated excitation intact). Also, the fact that population theta oscillations occur at all in such a pharmacologically and anatomically reduced system provides evidence for the existence of theta generating networks intrinsic to this brain region. Thus, rhythmic inputs from extra-ammonic regions (Petsche *et al.* 1962; Buzsáki *et al.* 1983; Vertes & Kocsis, 1997), though critical for the observation of theta activity in area CA1 *in vivo*, do not appear to impose their activity on an 'inert' network at theta frequencies.

Many of the properties of theta frequency oscillations in this reduced model match those seen in area CA1 *in vivo*. For example the sharp phase change seen in mid stratum radiatum in this model is also seen with 'atropine resistant' theta *in vivo* (Buzsáki *et al.* 1986). The pattern of activity in fast-spiking interneurons and the correspondence of pyramidal cell spiking (and its general sparsity) with the trough in stratum pyramidale field potentials also matches that seen *in vivo* (Fox *et al.* 1986; Bragin *et al.* 1995; Harris *et al.* 2000). However, a greater degree of temporal separation was seen between pyramidal interneuron spiking and oriens interneuron spiking in this model than reported for theta oscillations *in vivo* (Csicsvari *et al.* 1999). Atropine resistant theta oscillations *in vivo* also appear to be blocked by antagonists of the NMDA receptor (Vanderwolf & Leung, 1983), and field theta oscillations have been shown to be accompanied by dendritic electrogenesis (Kamondi *et al.* 1998).

In addition, the present observations showing the compartmental specificity of gamma and theta rhythms (Figs 1 and 3) suggest that large inputs from perisomatically targetted inhibitory synapses (as seen during field gamma oscillations) functionally isolate dendritic activity via perisomatic shunting (see Buzsáki, 2002). Assuming a passive propagation of dendritic IPSPs to the soma, the expression of the IPSP will be dependent on the cable properties of the dendritic compartments between site of origin and soma. A barrage of gamma-frequency IPSPs on dendrites between the distal site of origin and the soma would be expected to change the length constant of the dendrite dynamically, thus disrupting the fidelity of distal dendritic events as seen at the soma. It is this barrage of perisomatic inhibition which is attenuated by AMPA receptor blockade in the present experiments, thus almost abolishing field gamma oscillations (see Fisahn *et al.* 1998; Traub *et al.* 2000). This suggested that, though dendritic theta frequency activity was 'on-going' during field gamma oscillations in the present models, perisomatic gamma activity was too large to express a theta frequency dipole in area CA1.

At least two types of stratum oriens dendrite-targetting interneurons have been shown to have intrinsic theta generating properties – oriens lacunosum moleculare (OLM) cells and bistratified cells (Maccaferri & McBain, 1996; T. Gloveli & E. H. Buhl, unpublished observations). Lacunosum moleculare (LM) interneurons have also been shown to generate theta frequency oscillations (Chapman & Lacaille, 1999) and may correspond to proposed theta generating interneurons described by others (e.g. Banks *et al.* 2000). However, these cells were not reported to require active I_h currents to generate intrinsic theta frequency oscillations and so may not play a major role in the oscillations demonstrated by the present model (see Fig. 4). OLM interneurons demonstrate action potential generation that is sensitive to ZD7288 (Maccaferri & McBain, 1996) and appear to target apical dendrites more distally than the profile of perisomatic inhibitory input reported (Buhl *et al.* 1994; Papp *et al.* 2001). I_h has also been reported to be present in pyramidal dendrites where it is tonically active at resting membrane potentials (Magee, 1998). We cannot exclude, therefore, the possibility that the effects of ZD7288 on field theta oscillations may also be due to direct effects on pyramidal dendritic electrogenesis. However, we demonstrated here that blockade of dendritic activity with nickel ions appeared not to affect the pattern of theta frequency IPSP trains in pyramidal cells whereas bath application of ZD7288 did.

A critical role for the generation of field theta oscillations by these oriens interneurons was suggested by their firing

relationship with respect to both pyramidal neuronal somatic and dendritic IPSP profiles and fast spiking stratum pyramidale interneuron spiking (Fig. 9). The compound somatic IPSPs seen during field theta oscillations took the form of an initial large IPSP peaking some 12 ms before the peak of one period of the field oscillation. Given that the mean rise time of these IPSPs was *ca* 6 ms this suggested that these somatic IPSPs began approximately 6 ms after the mean action potential generation time for oriens theta cells during one theta period. During the initial decay phase of these IPSPs a distinct 'hump' is often seen corresponding temporally to the generation of dendritic spikes (the peak of the stratum pyramidale field). Following this the apparent decay of the IPSP is prolonged owing to a barrage of small IPSPs which temporally correlated with the trains of fast spiking stratum pyramidale interneurons recorded. Pyramidal somatic recordings showed almost no action potential generation during this theta model but small depolarisations generated spikes at the tail of this train of small IPSPs (i.e. approximately in antiphase with dendritic spiking). This system, as apparent from present data, may go some way towards explaining the discrepancy between pyramidal spike timing and excitatory and inhibitory inputs during theta *in vivo* (see Buzsáki, 2002 for discussion).

A number of dendritic calcium channels have been suggested to play a role in generating or shaping theta oscillations (e.g. Kamondi *et al.* 1998). Here we have demonstrated that the dendritic compartment of CA1 pyramidal cells may generate Ni^{2+}-dependent spikes at theta frequencies during a field theta oscillation. The pharmacological and electrophysiological profile of these spikes indicated activation of T-type (or P/Q) calcium channels in dendrites (e.g. see Magee *et al.* 1995). Ni^{2+} has also been shown to block synaptic plasticity induced by theta-burst stimulation (Ito *et al.* 1995) suggesting that these dendritic spikes not only contribute critically to the expression, as a field potential, of theta rhythmogenesis but may also play a role in synaptic plastic processes occurring at theta frequencies. The timing of individual pyramidal dendritic spikes, relative to the population theta oscillation, was exquisitely sensitive to dendritic depolarisation (see also Magee, 2001). Such depolarisation would be expected with entorhinal inputs and may be involved in the dynamic changes in pyramidal cell activity with behaviour *in vivo* (O'Keefe & Recce, 1993).

In summary, type I mGluR activation in area CA1 of the hippocampal slice generated theta frequency intracellular dendritic oscillations in pyramidal cells. Blockade of AMPA receptor-mediated glutamatergic excitation exposed a population theta oscillation in all CA1 laminae. The resulting population theta rhythm resembled atropine-resistant theta oscillations recorded *in vivo* and may be generated by a subset of stratum oriens interneurons possessing intrinsic membrane potential oscillations at theta frequency. Theta frequency oscillations showed a compartmental profile in pyramidal neurons different to that seen for gamma oscillations with dendritic or somatic depolarisation having markedly different effects on the temporal aspects of pyramidal neuronal electrogenesis.

REFERENCES

Awad, H., Hubert, G. W., Smith, Y., Levey, A. I. & Conn, P. J. (2000). Activation of metabotropic glutamate receptor 5 has direct excitatory effects and potentiates NMDA receptor currents in neurons of the subthalamic nucleus. *Journal of Neuroscience* **20**, 7871–7879.

Banks, M. I, White, J. A. & Pierce, R. A. (2000). Interactions between distinct $GABA_A$ circuits in hippocampus. *Neuron* **25**, 449–457.

Bragin, A., Jando, G., Nadasdy, Z., Hetke, J., Wise, K. & Buzsáki, G. (1995). Gamma frequency (40–100 Hz) patterns in the hippocampus of the behaving rat. *Journal of Neuroscience* **15**, 47–60.

Buhl, E. H., Halasy, K. & Somogyi, P. (1994). Diverse sources of hippocampal unitary inhibitory postsynaptic potentials and the number of synaptic release sites. *Nature* **368**, 823–828.

Buzsáki, G. (1989). Two-stage model of memory trace formation: a role for 'noisy' brain states. *Neuroscience* **31**, 551–570.

Buzsáki, G. (2002). Theta oscillations in the hippocampus. *Neuron* **33**, 325–340.

Buzsáki, G., Czopf, J., Kondakor, J. & Kellenyi, L. (1986). Laminar distribution of hippocampal rhythmic slow activity (RSA) in the behaving rat; current source density analysis, effects of urethane and atropine. *Brain Research* **365**, 125–137.

Buzsáki, G., Leung, L. & Vanderwolf, C. H. (1983). Cellular bases of hippocampal EEG in the behaving rat. *Brain Research Reviews* **6**, 139–171.

Chapman, C. A. & Lacaille, J. C. (1999). Cholinergic induction of theta-frequency oscillations in hippocampal inhibitory interneurons and pacing of pyramidal cell firing. *Journal of Neuroscience* **19**, 8637–8645.

Cobb, S. R., Buhl, E. H., Halasy, K., Paulsen, O. & Somogyi, P. (1995). Synchronisation of neuronal activity in hippocampus by individual GABAergic interneurons. *Nature* **378**, 75–78.

Cobb, S. R., Butlers, D. O. & Davies, C. H. (2000). Coincident activation of mGluRs and MachRs imposes theta frequency patterning on synchronised network activity in the hippocampal CA3 region. *Neuropharmacology* **23**, 1933–1942.

Csicsvari, J., Hirase, H., Czurko, A., Mamiya, A. & Buzsáki, G. (1999). Oscillatory coupling of hippocampal pyramidal cells and interneurons in the behaving rat. *Journal of Neuroscience* **19**, 274–287.

Fisahn, A., Pike, F. G., Buhl, E. H. & Paulsen, O. (1998). Cholinergic induction of network oscillations at 40 Hz in the hippocampus *in vitro*. *Nature* **394**, 186–189.

Fox, S. E., Wolfson, S. & Ranck, J. B. Jr (1986). Hippocampal theta rhythm and the firing of neurons in walking and urethane anaesthetised rats. *Experimental Brain Research* **62**, 495–508.

Harris, K., Henze, D. A., Hirase, H., Csicsvari, J. & Buzsáki, G. (2000). The accuracy of tetrode spike separation as determined by simultaneous intracellular and extracellular measurements. *Journal of Neurophysiology* **84**, 401–414.

Isomura, Y., Fujiwara-Tsukamoto, Y., Imanishi, M., Nambu, A. & Takada, M. (2002). Distance-dependent Ni^{2+}-sensitivity of synaptic plasticity in apical dendrites of hippocampal CA1 pyramidal cells. *Journal of Neurophysiology* **87**, 1169–1174.

Ito, K., Miura, M., Furuse, H., Zhixiong, C., Kato, H., Yasutomi, D., Inoue, T., Kikoshiba, K., Kimura, T., Sakakibara, S. & Miyakawa, H. (1995). Voltage-gated Ca^{2+} channel blockers, omega-AgaIVA and Ni^{2+}, suppress the induction of theta-burst induced long-term potentiation in guinea-pig hippocampal CA1 neurons. *Neuroscience Letters* **183**, 112–115.

Kamondi, A., Acsady, L. & Buzsáki, G. (1998). Dendritic spikes are enhanced by cooperative network activity in the intact hippocampus. *Journal of Neuroscience* **18**, 3919–3928.

King, C., Recce, M. & O'Keefe, J. (1998). The rhythmicity of cells of the medial septum/diagonal band of Broca in the freely moving rat: relationships with behaviour and hippocampal theta. *European Journal of Neuroscience* **10**, 464–477.

Larson, J. & Lynch, G. (1986). Induction of synaptic potentiation in hippocampus by patterned stimulation involves two events. *Science* **232**, 985–988.

Maccaferri, G. & McBain, C. (1996). The hyperpolarization-activated current (I_h) and its contribution to pacemaker activity in rat CA1 hippocampal stratum oriens-alveus interneurones. *Journal of Physiology* **497**, 119–130.

Maccaferri, G., Roberts, J. D., Szucs, P., Cottingham, C. & Somogyi, P. (2000). Cell surface domain specific postsynaptic currents evoked by identified GABAergic neurones in rat hippocampus *in vitro*. *Journal of Physiology* **524**, 91–116.

MacVicar, B. A. & Tse, F. W. Y. (1989). Local neuronal circuitry underlying cholinergic rhythmical slow activity in CA3 area of rat hippocampal slices. *Journal of Physiology* **417**, 197–212.

Magee, J. C. (1998). Dendritic hyperpolarisation-activated currents modify the integrative properties of hippocampal CA1 pyramidal neurons. *Journal of Neuroscience* **18**, 7613–7624.

Magee, J. C. (2001). Dendritic mechanisms of phase precession in hippocampal CA1 pyramidal neurons. *Journal of Neurophysiology* **86**, 528–532.

Magee, J. C., Christofi, G., Miyakawa, H., Christie, B, Lasser-Ross, N. & Johnston, D. (1995). Subthreshold synaptic activation of voltage-gated calcium channels mediates a localised calcium influx into the dendrites of hippocampal pyramidal neurons. *Journal of Neurophysiology* **74**, 1335–1342.

O'Keefe, J. & Nadel, L. (1978). *The Hippocampus as a Cognitive Map*. Clarendon, Oxford.

O'Keefe, J. & Recce, M. L. (1993). Phase relationship between hippocampal place units and the EEG theta rhythm. *Hippocampus* **3**, 317–330.

Papp, E., Leinekugel, X., Henze, D. A., Lee, J. & Buzsáki, G. (2001). The apical shaft of CA1 pyramidal cells is under GABAergic interneuronal control. *Neuroscience* **102**, 715–721.

Petsche, H., Stumpf, C. & Gogolak, G. (1962). The significance of the rabbit's septum as a relay station between midbrain and the hippocampus I. The control of hippocampus arousal activity by septum cells. *Electroenchephalography and Clinical Neurophysiology* **450**, 127–142.

Traub, R. D., Bibbig, A, Fisahn, A., LeBeau, F. E. N., Whittington, M. A. & Buhl, E. H. (2000). A model of gamma-frequency network oscillations induced in the rat CA3 region by carbachol *in vitro*. *European Journal of Neuroscience* **12**, 4093–4106.

Traub, R. D., Miles, R. & Buzsáki, G. (1992). Computer simulation of carbachol-driven rhythmic population oscillations in the CA3 region of the *in vitro* rat hippocampus. *Journal of Physiology* **451**, 653–672.

Vanderwolf, C. H. & Leung, L. S. (1983). Hippocampal rhythmical slow activity: a brief history and effects of entorhinal lesions and phencyclidine. In *The Neurobiology of the Hippocampus,* ed. Siefert, W., pp. 275–302. Academic Press, London.

van Hooft, J. A., Guiffrida, R., Blatow, M. & Monyer, H. (2000). Differential expression of group I metabotropic glutamate receptors in functionally distinct hippocampal interneurons. *Journal of Neuroscienc,* **20**, 3544–3551.

Vertes, R. P. & Kocsis, B. (1997). Brainstem-dienchephalo-septohippocampal sytems controlling the theta rhythm of the hippocampus. *Neuroscience* **81**, 893–926.

Whittington, M. A., Traub, R. D. & Jefferys, J. G. (1995). Synchronized oscillations in interneuron networks driven by metabotropic glutamate receptor activation. *Nature* **373**, 612–615.

Williams, J. H. & Kauer, J. A. (1997). Properties of carbachol-induced oscillatory activity in rat hippocampus. *Journal of Neurophysiology,* **78**, 2631–2640.

Acknowledgements

This work was supported by The Medical Research Council and The Wellcome Trust. M. Gillies is in receipt of an MRC CASE studentship in conjuction with GlaxoSmithKline plc.